Jurnal Mekanikal
Disember 2004, Bil.18 , 46 – 65

PREDICTION OF MOTION CHARACTERISTICS ON SWATH TYPE FLOATING STRUCTURE USING TWO-DIMENSIONAL FRANK CLOSE-FIT TECHNIQUE

Mas Murtedjo
Eko B. Djatmiko

Senior Lecturer, Department of Ocean Engineering
Faculty of Marine Technology - Sepuluh Nopember Institute of Technology (ITS)
ITS Campus - Sukolilo, Surabaya 60111 – Indonesia
Phone/Fax: +62 (031) 5928105
E-mail: citramas@sby.dnet.net.id
mas@oe.its.ac.id

ABSTRACT

The unique shape of SWATH which consists of two submerged hulls connected to the cross deck via slender struts has brought an excellent sea keeping quality. This makes an extensive study on the SWATH motion characteristics an important part in its design process. This paper describes the utilization of mathematical model to predict such vessel motions based on the Frank Close-Fit technique combined with the well-known 2-D strip theory. This technique was applied to compute the radiation, incident wave excitation and diffraction components. These three components are then substituted into 5-DOF differential equations for SWATH motion in regular wave to attain its motion responses, namely sway, heave, roll, pitch, and yaw. SWATH motions were identified due to beam sea (90°), quartering sea (135°) and head sea (180°). The results of computation generally are in good agreement with experimental data. Certain discrepancies, especially in the peak value of roll motion are primarily brought about the absence of viscous damping. Slight discrepancies in the horizontal mode of motions, namely surge and yaw, are identified due to the harnesses effect applied to the physical model. It may be concluded at this stage that the mathematical model is considered appropriate to be applied in the preliminary design of SWATH type vessels.

Keywords: *SWATH, Frank Close Fit-technique, 2-D strip theory, sway, heave, roll, pitch, yaw, beam sea, quartering sea, head sea*

1.0 INTRODUCTION

SWATH (Small Waterplane-Area Twin-Hull) type vessel may be utilized in various ocean engineering activities, namely as supply vessels, oceano-hydrographic research vessels, also as supporting facilities of offshore drilling rigs.

The idea of SWATH concept development is to produce floating structure, which is capable to maintain low motion characteristics when operating in relatively severe seas, without any significant speed degradation, slamming and

shipping of green water. This concept is met by designing a twin-hulled floating structure. Each hull comprises of two parts, namely the strut and the submerged hulls. The strut basically is a slim body shape located at the air and water surface intersection. SWATH could be designed with a single or tandem strut per hull. The submerged hull, which contains a large portion of the buoyant volume, is positioned well below the sea wave effect, commonly configured as a torpedo body shape. The struts at certain distance above the sea level support the primary deck and superstructure; so that slamming and shipping of green sea effect can be reduced. The primary deck normally has a simple rectangular section, the bottom of which is longitudinally contoured at the fore and aft ends. The twin hull configuration implies that the vessel has an ample hydrostatic restoring moment. This is similar to conventional catamaran but with a difference in the hull shape. A typical SWATH configuration, including the main parameters, may be shown as in Figure 1.

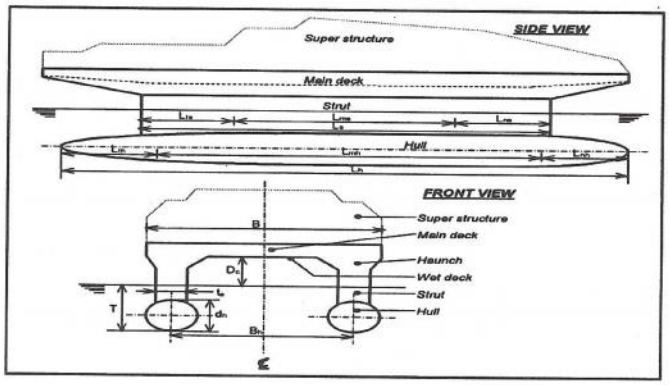

Figure 1 Typical configuration and main parameters of the floating body of SWATH type

The shape of SWATH hull makes the wave excitation force smaller compared to conventional monohull vessel or catamaran. The configuration of the strut brings waterline area smaller than conventional vessel, so SWATH natural periods are characteristically much longer in comparison to the periods of conventional monohull ships. This implies that the large amplitude of motions due to resonance could be safely avoided. Lower motion in sea waves assures the vessel to be able of sailing with minimum speed degradation, as well as less probability of slamming and shipping of green waters. It is obvious from the discussion above that SWATH is competitive in view of its serene motion characteristics. A comprehensive study on its motion is therefore necessary, especially to achieve an optimum design. Such a study has been performed, as explained in this paper.

In the first stage discussion is focused on the application of the 2-D strip theory in combination with the Frank Close-Fit technique to develop the

mathematical model of SWATH motion, especially in identifying the effect of radiation, incident wave and diffraction wave components. The mathematical model was then employed to predict the motion characteristics (motion response amplitude operators) of SWATH due to the variations of wave height, wave frequency, SWATH advancing speed, and the wave directions (head sea, beam sea and quartering sea). Finally, to find the validation, results of the mathematical model are compared to the data derived from physical model testing at hydrodynamic laboratory.

2.0 MATHEMATICAL MODEL FOR SWATH MOTION

As for the case of hydrodynamic analysis on other floating structures, basically there are three methods available for predicting the motion of SWATH type vessels. These methods are: a) Morrison equation, b) 2-D strip theory, and c). 3-D diffraction theory.

The use of Morrison equation on a number of offshore structures may be acceptable if certain assumptions are satisfied [1]. The primary assumption is that the size of the structure is relatively small, i.e. less than 20% of the wave length. This assumption appropriate only when considering the slender strut under excitation of waves at a peculiar direction. Nonetheless, the relatively larger size of the submerged SWATH hulls restricts the accuracy of prediction by applying this method [2]. Problem solving by the application of the 2-D strip theory, according to many publications, may be carried out by two approaches. The first approach is related to the adoption of multiple expansion technique and the second is by the use of Frank close-fit technique.

In applying the multiple expansion technique, flow around submerged structure is principally modeled by singularity divergence. It can either be source or doublet distributed on the structure axis. If the longitudinal section has different shape, then the singularity distribution on the vertical direction must be done by relatively short interval, which means more iteration should be executed, hence computational time will be longer. If the interval is not short enough, then the numerical stability in the computation usually could not be well gained. This technique firstly developed for single hull vessel by Nondenstorm [3], and adapted for floating structure SWATH type by Lee and Curphey [4], which until now are considered as the pioneers in the hydrodynamics research of that type of floating structure. The enhancement of the findings has been done by several other researchers like Hong [5], Fang [6] and Kobayashi et. al. [7].

The second technique was based on the method as introduced by Frank [8] for ordinarily configured body and then expanded for single hull vessel. In this technique, singularity distribution is done on the body surface which is divided into a number of segments closely represents the shape, therefore it is referred to as the Close-Fit. By this technique, a theoretically unlimited analysis can be made for the circular shaped configuration. The accuracy of the computation of course

then depends on the number of segments along the body surface is made. More complicated surface configuration normally needs more segmentations. Frank Close-Fit Technique has been adapted by Atlar et al. [9] to be used on the analysis of floating structure motion of semi-submersible and SWATH types.

2.1 SWATH Motion Equation

Prior to the derivation of motion equation, it needs to know first about the coordinate system, which is used. As shown in Figure 2 below the coordinate system consists of:

a. *O-Xo, Yo, Zo* coordinate, fixed on the space and on still water level.
b. *G-x, y, z* coordinate, fixed on the body of SWATH and its origin point was precisely at the centre of gravity.

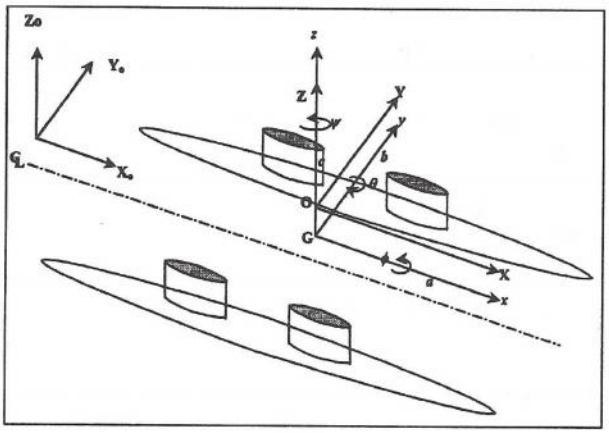

Figure 2 Coordinate system and the definition of vessel motions

Further, as defined in Figure2, the six modes of the vessel motion are divided into the translational motions, i.e. surging (x); swaying (y); and heaving (z), and the rotational motions, i.e. rolling (ϕ); pitching (θ); and yawing (ψ). The corresponding six-degree of freedom motion equation in sinusoidal wave are given by the following differential equation:

$$\sum_{k=1}^{6}(M_{jk}+A_{jk})\ddot{S}_k+B_{jk}\dot{S}_k+C_{jk}s_k=F_j \qquad (1)$$

where: k = kind of motion; j = kind of excitation; M_{jk} = matrix of mass; A_{jk} = matrix of added mass; B_{jk} = matrix of damping; C_{jk} = matrix of restoring component; S_k = motion displacement vector for one wave amplitude; and F_j = force vector and wave excitation moment for one wave amplitude.

Force vector and wave excitation moment on the right hand side of the equation (1) can be expressed into complex function as follows:

$$Fj = \left\{(F_{jR} + iF_{jR})e^{-i\omega t}\right\} = F_{jR}\cos\omega t + F_{jR}\sin\omega$$

$$= \left|F_j\right|\cos((\varepsilon_j - \omega t) \tag{2}$$

where: $$\left|F_j\right| = \sqrt{\left(F_{jR}^2 + F_{jI}^2\right)} \tag{3}$$

= maximum wave excitation force

F_{jR} = real part of wave excitation force

F_{jI} = imaginary part of wave excitation force

ε_j = arctan (F_{jI}/F_{jR}) (4)

= phase angle when wave excitation force is maximum

Similar to the expression Fj in complex form, then motion displacement is also expressed in complex function:

$$S_k = \mathrm{Re}\left\{\overline{S_k}e^{-i\omega t}\right\} \tag{5}$$

So, the velocity and acceleration components are given by:

$$\dot{S}_k = -i\omega\overline{S_k}e^{-i\omega t} \tag{6}$$

$$\ddot{S}_k = -\omega^2\overline{S_k}e^{-i\omega t} \tag{7}$$

Applying expression in equation (2) up to equation (7), the motion displacement can be written as:

$$\overline{S_k} = S_{kR} + iS_{kI} = S_{kR}\cos\omega t + S_{kI}\sin\omega t$$

$$\left|S_k\right| = cos(\alpha_k - \omega t) \tag{8}$$

or

$$\left|S_k\right| = \sqrt{\left(S_{kR}^2 + S_{kI}^2\right)} \tag{9}$$

and

$$\alpha_k = arctan\ (S_{kI}/S_{kR}) \tag{10}$$

where:

$|S_k|$ = maximum motion displacement
S_{kR} = real part of motion displacement
S_{kI} = imaginary part of motion displacement
α_k = phase angle when maximum motion displacement occurs

2.2 The Solution of Motion Equation

The surge motion is assumed as an uncoupled motion, so its effect on other motions does not exist. Further, the added mass, damping and diffraction wave force along x–axis was considered too small, so it can be ignored. Therefore, having the above assumption, the surge motion on that condition can be solved as follows:

$$M \ddot{x} = F_1 \tag{11}$$

Or by making the coordinate system as a reference, equation (11) can be expressed as:

$$(M_{55} + A_{55})\ddot{S}_5 + B_{55}\dot{S}_5 + C_{55}S_5 + A_{53}\ddot{S}_3 + B_{53}\dot{S}_3 + C_{53}S_3 = F_5 \tag{12}$$

Symmetric hull with the reference to centre plane can caused a couple motion between the vertical plane motions (heave and pitch) with the horizontal plane motion (sway, roll, yaw). So the motion equation can be divided into two groups. By making expansion to equation (1) for heave and pitch, where $j, k = 3$ & 5, so it can be written:

$$(M_{33} + A_{33})\ddot{S}_3 + B_{33}\dot{S}_3 + C_{33}S_3 + A_{35}\ddot{S}_5 + B_{35}\dot{S}_5 + C_{35}S_5 = F_3 \tag{13}$$

Or by using coordinate system, equation (13) can be expressed as:

$$\begin{aligned}(M_{33} + A_{33})\ddot{Z} + B_{33}\dot{Z} + C_{33}Z + A_{35}\ddot{\theta} + B_{35}\dot{\theta} + C_{35}\theta &= F_3 \\ (I_5 + A_{55})\ddot{\theta} + B_{55}\dot{\theta} + C_{55}\theta + A_{53}\ddot{Z} + B_{53}\dot{Z} + C_{53}Z &= F_5\end{aligned} \tag{14}$$

By making expansion to equation (1) the equation of motions of sway, roll and yaw, where $j, k = 2$, 4 and 6, can be written:

$$\begin{aligned}(M_{22} + A_{22})\ddot{S}_2 + B_{22}\dot{S}_2 + A_{24}\ddot{S}_4 + B_{24}\dot{S}_4 + A_{26}\ddot{S}_6 + B_{26}\dot{S}_6 &= F_2 \\ (M_{44} + A_{44})\ddot{S}_4 + B_{44}\dot{S}_4 + C_{44}S_4 + A_{12}\ddot{S}_2 + B_{42}\dot{S}_2 + A_{46}\ddot{S}_6 + B_{46}\dot{S}_6 &= F_4 \\ (M_{66} + A_{66})\ddot{S}_6 + B_{66}\dot{S}_6 + A_{62}\ddot{S}_2 + B_{62}\dot{S}_2 + A_{64}\ddot{S}_4 + B_{64}\dot{S}_{46} &= F_6\end{aligned} \tag{15}$$

Or by using coordinate system, eq (15) can be expressed as:

$$(M + A_{22})\ddot{y} + B_{22}\dot{y} + A_{24}\ddot{\Phi} + B_{24}\dot{\Phi} + A_{26}\ddot{\Psi} + B_{26}\dot{\Psi} = F_2$$
$$(I_4 + A_{44})\ddot{\Phi} + B_{44}\dot{\Phi} + C_{44}\Phi + A_{42}\ddot{y} + B_{42}\dot{y} + A_{46}\ddot{\Psi} + B_{46}\dot{\Psi} = F_4$$
$$(I_6 + A_{66})\ddot{\Psi} + B_{66}\dot{\Psi} + A_{62}\ddot{y} + B_{62}\dot{y} + A_{64}\ddot{\Phi} + B_{64}\dot{\Phi} = F_6 \qquad (16)$$

2.3 Froude-Krylov Force Component

When the structure was in local coordinate (*G-x, y, z*) moving forward with constant velocity, incoming wave potential will be the same as if the velocity is zero, except for encounter frequency change. By using matrix notation, the Froude-Krylov force for one wave amplitude, $f^k_{(m)}$ on the moving space can be expressed as:

$$\begin{bmatrix} f^k_{(2)}(x) \\ f^k_{(3)}(x) \\ f^k_{(4)}(x) \end{bmatrix} = \rho g \int_{s(x)} e^{k_o z} \begin{bmatrix} \sin \\ \cos \\ \sin \end{bmatrix} (k_o y \sin \mu) \begin{bmatrix} -dz \\ dy \\ ydy + (z - z_o)dz \end{bmatrix} \qquad (17)$$

where: ρ = sea water density.

Force integration along the SWATH length and computation wave phase angle will produce Froude-Krylov force per one wave amplitude, $F^k_{(m)}$, as in the following:

$$\begin{bmatrix} F^K_{(2)} \\ F^K_{(3)} \\ F^K_{(4)} \\ F^K_{(5)} \\ F^K_{(6)} \end{bmatrix} = \int_L e^{ik_o x \cos \mu} \begin{bmatrix} if^K_{(2)} \\ if^K_{(3)} \\ if^K_{(4)} \\ if^K_{(3)} \\ if^K_{(2)} \end{bmatrix} \begin{bmatrix} dx \\ dx \\ dx \\ -xdx \\ xdx \end{bmatrix} \qquad (18)$$

2.4 Diffraction Force Component

Force and excitation moment for sway, heave and roll motions caused by diffraction, $f^D_{(m)}$ can be expressed in the following matrix form:

$$\begin{bmatrix} f^D_{(2)}(x) \\ f^D_{(3)}(x) \\ f^D_{(4)}(x) \end{bmatrix} = i\rho\omega \int_{s(x)} e^{k_o z} \begin{bmatrix} \phi^{(0)}_D(y,z,k,\mu) \\ \phi^{(e)}_D(y,z,k,\mu) \\ \phi^{(0)}_D(y,z,k,\mu) \end{bmatrix} \begin{bmatrix} -dz \\ dy \\ y = dy + (z - z_o)dz \end{bmatrix} \qquad (19)$$

where:

$\phi_D{}^{(o)}$ = diffraction potential velocity in odd complex function

$\phi_D{}^{(e)}$ = diffraction potential velocity in even complex function

Diffraction velocity potential, ϕ_D can be expressed in the Green function and complex source strength by using normal differentiation of the following equation:

$$\frac{\partial}{\partial n}\phi_D^{(m)} = \left[\sum_{j=1}^{N} Q_j^{(m)} I_{ij}^{(m)} + \sum_{j=1}^{N} Q_{N+j}^{(m)} J_{ij}^{(m)}\right] + i\left[\sum_{j=1}^{N} Q_j^{(m)} J_{ij}^{(m)} - \sum_{j=1}^{N} Q_{N+j}^{(m)} I_{ij}^{(m)}\right] \quad (20)$$

where:

Q_j = Green function on j segment
I_{ij}, J_{ij} = influence coefficient.

By separating the right side and the left side of equation (20) into real and imaginer part, the odd function can then be expressed as:

$$\sum_{j=1}^{N} Q_j^{(m)} I_{ij}^{(m)} + \sum_{j=1}^{N} Q_{N+j}^{(m)} J_{ij}^{(m)} \quad (21)$$

and for the even function:

$$\sum_{j=1}^{N} Q_j^{(m)} J_{ij}^{(m)} - \sum_{j=1}^{N} Q_{N+j}^{(m)} I_{ij}^{(m)} \quad (22)$$

The odd function, either for incoming wave or diffraction produces excitation force of heave motion, and the even function produces excitation force of sway and roll. By considering the phase angle, the whole force and diffraction moment per one wave amplitude, $F^D_{(m)}$ is:

$$\begin{bmatrix} F^D_{(2)} \\ F^D_{(3)} \\ F^D_{(4)} \\ F^D_{(5)} \\ F^D_{(6)} \end{bmatrix} = \begin{bmatrix} F^D_{(2)}(k) \\ F^D_{(3)}(k) \\ F^D_{(4)}(k) \\ F^D_{(5)}(k) \\ F^D_{(6)}(k) \end{bmatrix} + \begin{bmatrix} 0 \\ 0 \\ 0 \\ \frac{U}{i\omega} F^D_{(3)}(k) \\ -\frac{U}{i\omega} F^D_{(2)}(k) \end{bmatrix} + \Gamma \begin{bmatrix} f^D_{(2)}(x) \\ f^D_{(3)}(x) \\ f^D_{(4)}(x) \\ f^D_{(5)}(x) \\ f^D_{(6)}(x) \end{bmatrix} \quad (23)$$

where:

$$\Gamma = \frac{U}{i\omega} e^{ik_o x \cos \mu}$$

The first matrix element on the right side of equation (23), $F^D_{(m)}(k)$, does not depend on velocity but rather on the encounter frequency. The second matrix element depends on velocity, which only affect the pitch and yaw motions. The third matrix contains the diffraction terms for the SWATH ends, ie. stern and stem, in which x refers to the longitudinal distance from the origin of the

coordinate system. The total wave excitation force per one wave amplitude, which affects the floating structure of SWATH type, is gained by adding the Froude-Krylov force (equation 18) and diffraction force (equation 23).

2.5 The Equation Identification for Forward Speed

The (G-x, y, z) coordinate has the same position as (O-X, Y, Z) coordinate at $t = 0$ after the vessel move forward on X-axis with U constant velocity. The relation between the fix coordinate and translation coordinate can be expressed as:

$$X = x + U_t; \quad Y = y; \qquad Z = z \tag{24}$$

The relation between the wave frequency and the encounter frequency, ω_e can be given as follows:

$$\omega_e = \omega_o - U K_o \cos \mu \tag{25}$$

where:

ω_o = incoming wave frequency at zero speed
μ = the wave heading angle
k_o = wave number = ω_o^2/g, and
g = acceleration due to gravity

By referring to G-x, y, z coordinate, which is moving forward with constant velocity, then the incident wave potentials, is expressed as:

$$\phi_I (x, y, z, k_o, \mu, t) = \phi_I (y, z, k_o, \mu)\, e^{i(ko \cos \mu - \omega t)} \tag{26}$$

with

$$\phi_I (y, z, k_o, \mu) = - \frac{ig\varsigma_A}{\omega_o} e^{(k_o Z)} e^{(ik_o y \sin \mu)} \tag{27}$$

where ζ_A is the wave amplitude.

3.0 FRANK CLOSE-FIT TECHNIQUE

With the reference to the strip theory, SWATH is divided into several strips along its structure length and the hydrodynamic interaction between the strips in longitudinal direction was ignored. The velocity potential of the 2-dimensional fluids in each strip can be determined using Green formula, and accomplished this formula numerically by using Frank Close-Fit technique in order to attain the force applies to each strip.

a) Incoming wave has been diffracted by SWATH based on the assumption that SWATH remains on its fixed position. This is called Diffraction Problem.
b) After the body diffracts the wave, SWATH begins to oscillate sinusoidally in still water. This problem is called Radiation Problem.

These results in total potential velocity θ from the fluids are the superposition of the following potentials:

$$\theta(x, y, z; t) = \theta_I(x, y, z; t) + \theta_D(x, y, z; t) + \theta_R(x, y, z; t) \quad (28)$$

where:

θ_I = incoming wave potential
θ_D = diffracted wave potential
θ_R = radiation potential

The analysis of each 2-dimensional strip for the diffraction and radiation problem will be dealt separately. Formulation of velocity potential that is required by θ_R and θ_D for each strip is represented by Green function with the help of Green's formula. Green's formula application for double hull can be explained by referring to Figure 3, where a 2-dimensional section of SWATH hull is differentiated into two planes namely [9]:

a) (D') area that is positioned inside the plane that is enclosed by left and right hull contour $(S_s + S_t)$ and freeboard S_f at which the strut intersects.
b) Fluids area (D) which is located inside the plane that is enclosed by freeboard S_f and upper hull contour $(S_s + S_I)$, control surface S_t in infinite distance, and S_{ea} bed S_b.

If $P(x, y)$ is a fixed point in fluids plane (D) and σ is $P(x, y)$ distance from the moving point $Po(\xi, \eta)$ which taken as elementary segment ds at hull contour, so the velocity potential can be derived using the Green's formula as below:

$$\phi(P) = \frac{1}{2\pi} \int_{(s+s')} \left[G(P; P_o \frac{\partial \Phi(p_o)}{\partial V} - \frac{\partial G}{\partial V} \Phi \right] ds(P_o) \quad (29)$$

Numerical solution of equation (29) can be acquired by segmenting floating body surface, and distribute the source in each element, as shown in Figure 4.

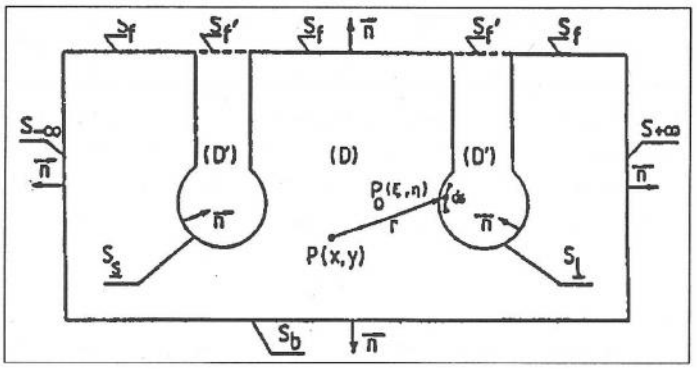

Figure 3 Mathematical definition of velocity potential determination at point Po due to the effect of P point

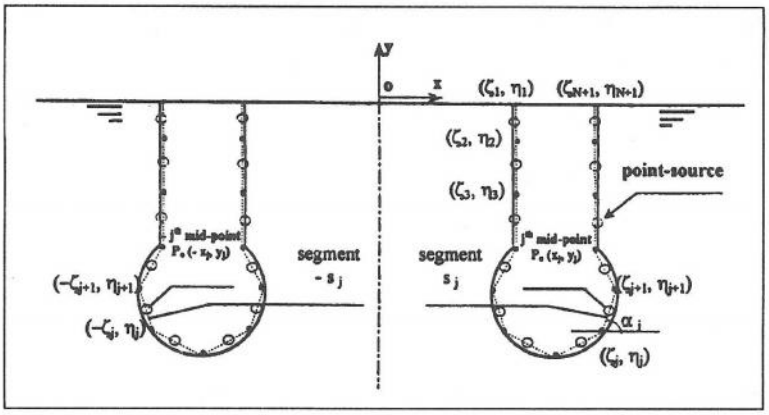

Figure 4 Double hull segmentation for Frank Close-Fit Technique application

For a symmetric double hull configuration, the problem can be simplified to consider only the hull at one side. Referring to Figure 4, the hull contour is divided into N segments by taking some $(N+1)$ points in hull contour $y_i(\xi_1, \eta_1)$, (ξ_2, η_2), $\ldots(\xi_{N+1}, \eta_{N+1})$. The point (ξ_{N+1}, η_{N+1}) is put on X-axis on the intersection between strut with the free water surface. The submerged hull is formed by connecting the $(N+1)$ points consecutively to represent the hull segment configured with straight lines which are identified as $j = 1,2,\ldots N$. If a source with a complex strength value of Q is put on a single point at each segment in order to acquired some $2N$ linear algebra equation as given in equations (21) and (22). These equations are then used for solving the above potential function numerically.

4.0 RESULTS OF THE ANALYSIS

The result of motion response calculation by the application of the 2-dimensional Frank Close-Fit technique in conjunction with the strip theory has been plotted together with the experimental data. The experimental data has been made available by [10]. The SWATH model for such a study is specified by the tandem strut configuration, with the ratio of hull length to diameter of 16.82 and the ratio of strut length to thickness of 11.15. The model draught is equivalent to twice of the hull diameter. The model has been tested in beam, quartering, and head seas at various wave frequencies and two different wave heights. The results of comparative evaluation between the theory and experiment are as outlined in the followings.

4.1 Beam Seas

The sway motion responses as depicted in Figure 5 shows a similar trend between the results of the strip theory and the experiment. For the low frequency region, the difference between the strip theory and the experiment results is quite notable.

Such a difference may be explained due to, firstly, the absence of viscous damping effect which are not taken into account in the theory. Secondly, during the test the model was harnessed to maintain its initial position. The presence of the harnesses could have restricted the sway oscillatory motion rather significantly. Hence the test results give lower amplitude than it was expected.

The theory and experiment shows a good agreement in heave motion response, as presented in Figure 6. In spite of this matter there is a little difference especially at non-dimensional maximum heave response zone. The theory could give more accurate results if the number of stations is increased. Maximum motion response value of non-dimensional heave response from the experiment is ± 2.65, whilst the maximum value from the theory is ± 2.0. For the roll motion response, as shown in Figure 7, both of experiment result and strip theory calculations are match one another. Only at the resonance frequency, a difference in maximum roll motion response is spotted. This occurs because water viscosity effect is not included in the computation.

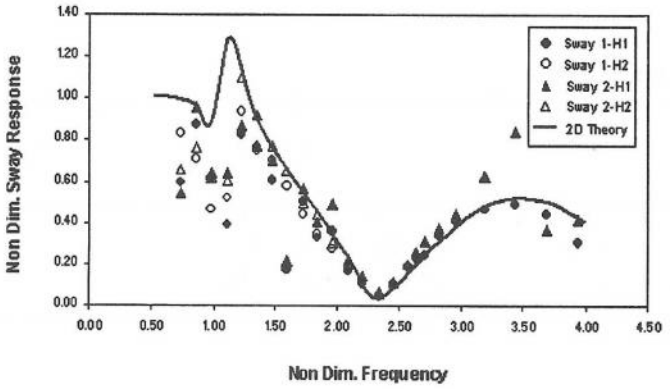

Figure 5 Non-Dimensional Sway Motion from SWATH-1 Model on regular wave at Beam Sea

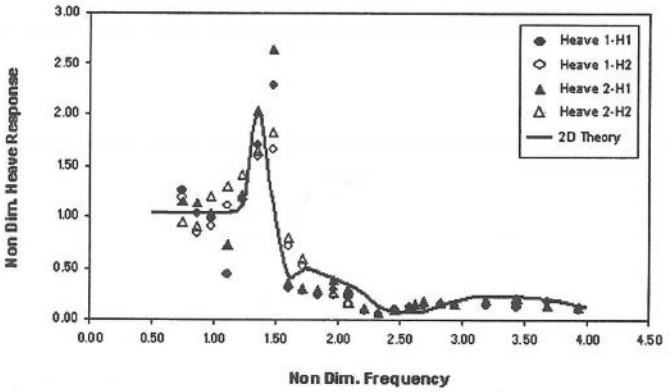

Figure 6 Non-Dimensional Heave Motion from SWATH-1 Model on regular Beam Sea

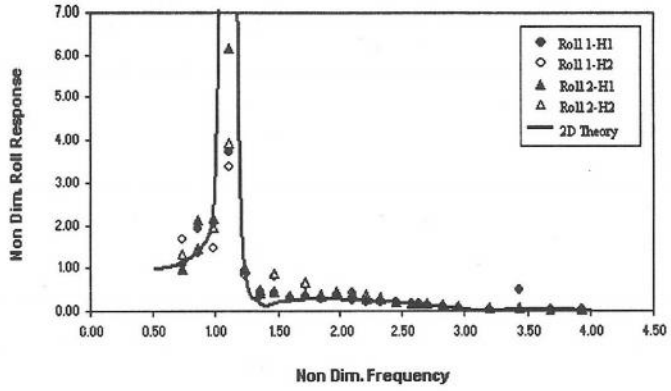

Figure 7 Non-Dimensional Roll Motion from SWATH-1 Model on regular Beam Sea

4.2 Quartering Seas

The results of sway motion response either yielded from the experiment or the strip theory indicates a quite similar graphical trend, as presented in Figure 8. However, it is obvious that the value of motion response from the two predictions differ quite significantly along the wave frequency range. Such a difference could be explained similar to that with the case in beam seas. It should be noted at this stage however; that the result from mathematical model seems to be the correct one, as the curve shows the pattern, which has the maximum value, approaches unity.

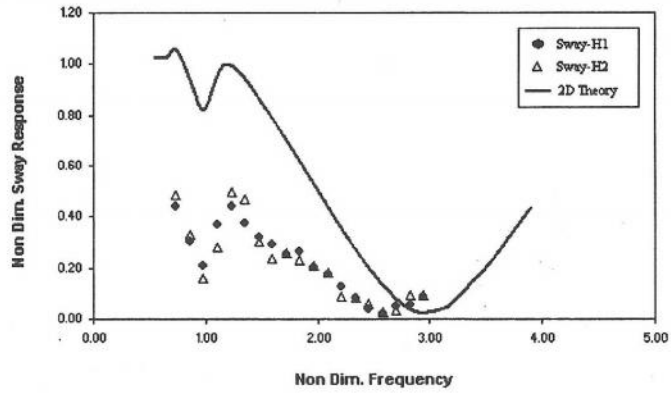

Figure 8 Non-Dimensional Sway Motion from SWATH-1 Model on regular Quartering Sea

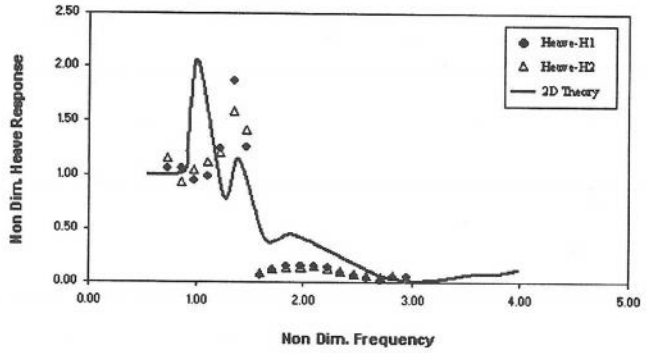

Figure 9 Non-Dimensional Heave Motion from SWATH-1 Model on regular Quartering Sea

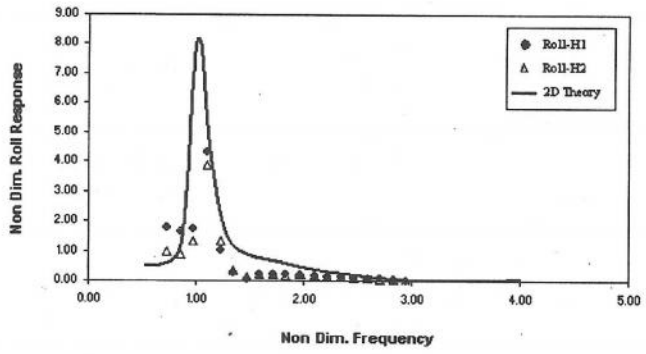

Figure 10 Non-Dimensional Roll Motion from SWATH-1 Model on regular Quartering Sea

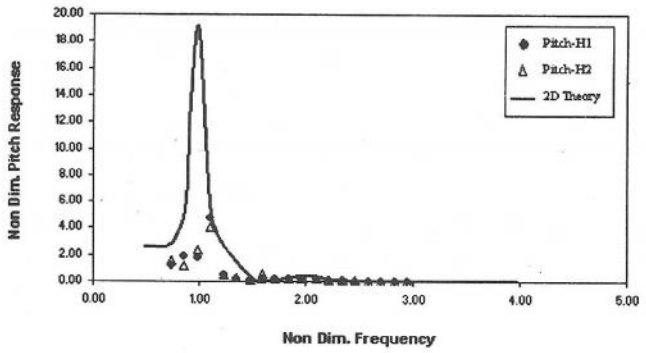

Figure 11 Non-Dimensional Pitch Motion from SWATH-1 Model on regular Quartering Sea

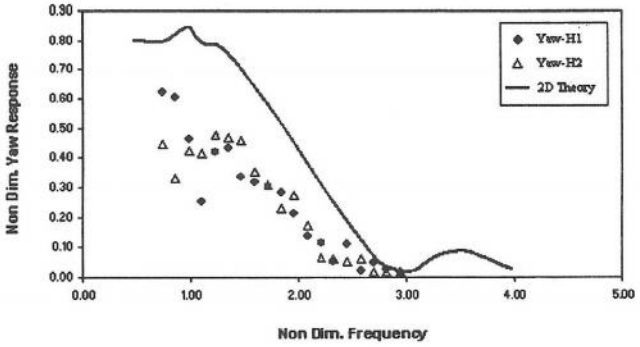

Figure 12 Non-Dimensional Yaw Motion from SWATH-1 Model on regular Quartering Sea

It is interesting to note that in Figure 9 the theory shows two distinguished peak for the response curve of the heave mode of motion in quartering seas. The first peak could be due to the substantial effect of roll motion on heave, as if one refer to the peak of the roll response curve in Figure 10. The second peak essentially the model own heave resonance. At higher frequency the theory, which does not taken into account the viscous damping, gives rather excessive value of response. The maximum heave response from both experiment and theory could reach as high as 2.0.

In the roll motion response as depicted in Figure 10, the strip theory calculation as well as experiment results give a similar graphical trend. However, motion response values have a quite significant difference especially at resonance frequency region. The absence of damping due to viscosity and wave reflection effect between the two same hulls are the factors that have possibly cause such a difference.

On the pitch motion response as shown in Figure 11, the strip theory calculations predict a similar trend as that attained by the experiment. But it is obvious that the value of motion response from the strip theory is substantially higher to the experiment result. Strip theory, which does not consider water viscosity factor, has caused to increase pitch motion response.

The difference in values and similarity in graphical trends of yaw motion response from the theory and experiment, as presented in Figure 12, are basically brought about by the tendency in sway motions. The explanation of the factors that has brought about such a difference therefore is the same as those for the case of sway motions.

4.3 Head Seas

For the head sea case the experiment has been performed for both stationary (V=0.0 m/s) and advancing speed conditions. For the advancing condition the model speed has been varied at four different values, namely V=0.5 m/s, 1.0 m/s,

1.5 m/s, and 2.0 m/s, which pertinently corresponds to the Froude number *Fn* of 0.13, 0.26, 0.39, and 0.52, respectively.

a. Stationary Condition

In this condition the strip theory calculation to the experiment results match very well for the case of heave motion responses, as exhibited in Figure 13. Whereas for the pitch motion response, as shown in Figure 14, the strip theory gives rather high values than that from the experiment. Again, the difference is due to the absence of viscous damping effect. Nonetheless, the difference is not so significant, and similar to that in the quartering sea cases.

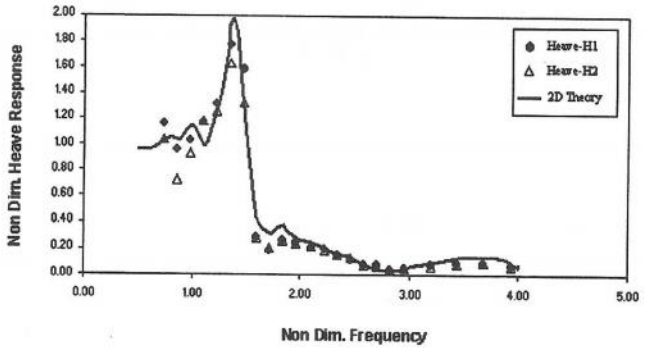

Figure 13 Non-Dimensional Heave Motion from SWATH-1 Model on regular Head Sea (V = 0 m/s; Fn = 0)

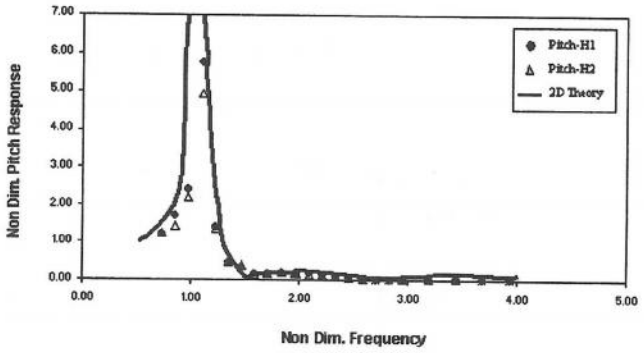

Figure 14 Non-Dimensional Pitch Motion from SWATH-1 Model on regular Head Sea (V = 0 m/s; Fn = 0)

b. Advancing Speed Condition

At four different advancing speeds the agreement between the theory and experiment in the heave motion response is obvious, as exhibited in Figs. 15 to 18. The only discrepancy is spotted at V=0.5 m/s or Fn=0.13, which could be brought about by lack of frequency input for the computation. In other words, the

frequency input interval should be shortened especially at the resonance frequency range. Considering Figs. 15 to 18, the maximum values of heave response for the model moving with forward speed could reach as high as 3.5. This is as expected, in which the heave responses should be higher when the vessel is moving with forward speed if compared to that in stationary conditions whether in beam, quartering or head seas.

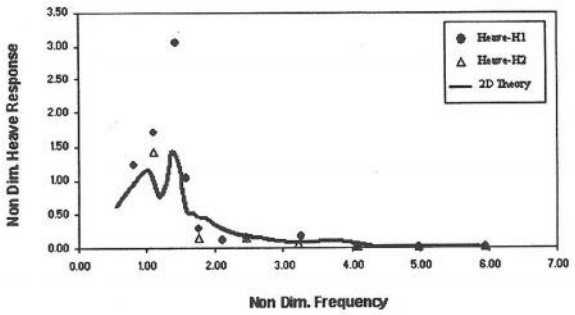

Figure 15 Non-Dimensional Heave Motion from SWATH-1 Model on regular Head Sea (V = 0.5 m/s; Fn = 0.13)

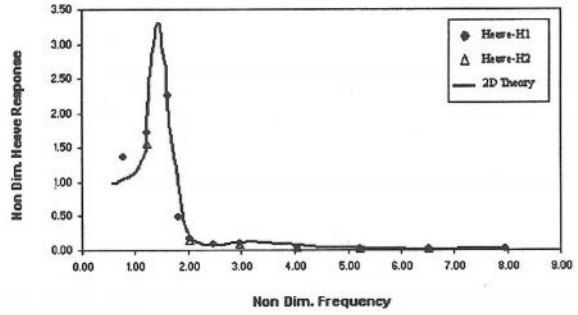

Figure 16 Non-Dimensional Heave Motion from SWATH-1 Model on regular Head Sea (V = 1.0 m/s; Fn = 0.26)

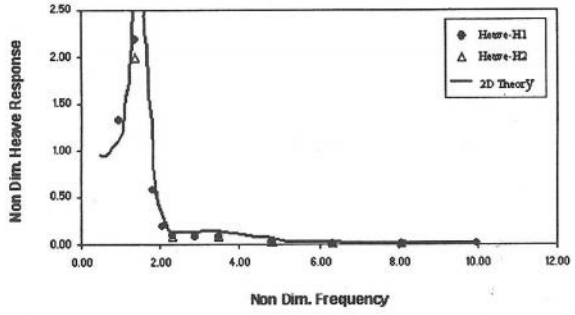

Figure 17 Non-Dimensional Heave Motion from SWATH-1 Model on regular Head Sea (V = 1.5 m/s; Fn = 0.39)

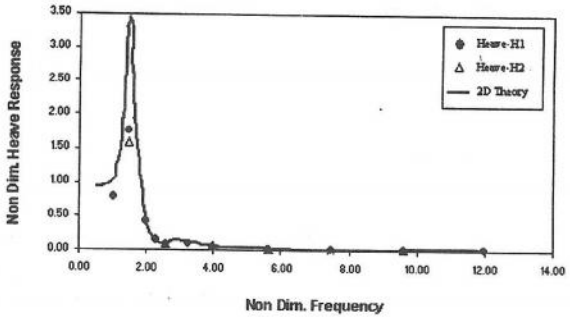

Figure 18 Non-Dimensional Heave Motion from SWATH-1 Model on regular Head Sea (V = 2.0 m/s; Fn = 0.52)

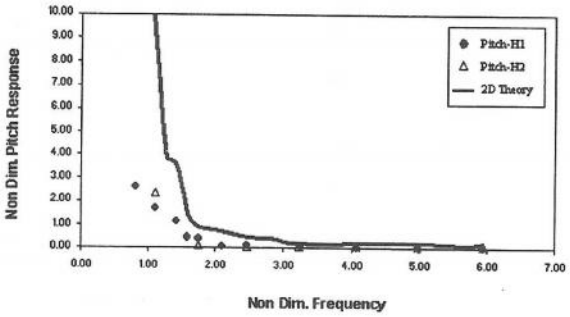

Figure 19 Non-Dimensional Pitch Motion from SWATH-1 Model on regular Head Sea (V = 0.5 m/s; Fn = 0.13)

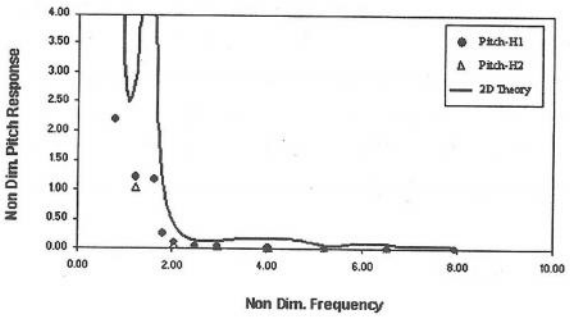

Figure 20 Non-Dimensional Pitch Motion from SWATH-1 Model on regular Head Sea (V = 1.0 m/s; Fn = 0.26)

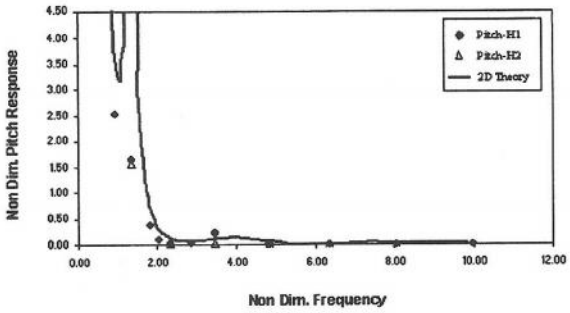

Figure 21 Non-Dimensional Pitch Motion from SWATH-1 Model on regular Head Sea (V = 1.5 m/s; Fn = 0.39)

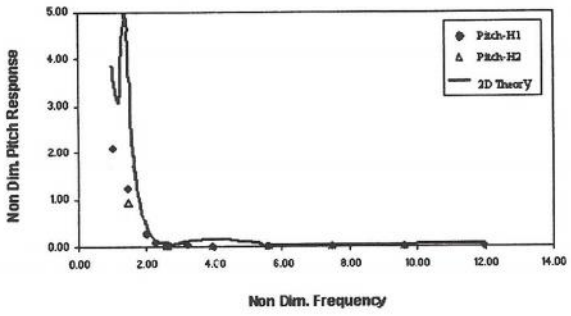

Figure 22 Non-Dimensional Pitch Motion from SWATH-1 Model on regular Head Sea (V = 2.0 m/s; Fn = 0.52)

For the pitch motion response, the strip theory and experiment results share a similar trend, especially in its amplification in line with the increasing of forward speed, as presented in Figures 19 to 22. The agreement in the pitch response values is obvious at supercritical regions. Nonetheless, in the critical and sub-critical zones the discrepancies are notable. These discrepancies is often caused by the over prediction of the coupled effect of heave to pitch motion, especially in critical or resonance frequency zone.

5.0 CONCLUSIONS

This paper presents the mathematical prediction of SWATH ship motions in regular waves, based of the Frank close-fit technique combined with the 2-dimensional strip theory. The results of the mathematical prediction have been verified in a comparative evaluation with experimental data. In general the theory shows fairly good agreement with experimental approach. Certain discrepancies, which are spotted, could have been primarily brought about the absence of

viscous damping in the mathematical prediction. In the second degree, the difference might have been caused by the effect of harnesses that have been applied during the model test. In case of model with forward speed condition, difference in pitch responses presumably was developed due to the over prediction in the coupled heave-pitch motion effects.

Refinement of the mathematical model is on going at present, especially to consider the viscous damping effect and scrutinizing the accuracy of coupled heave-pitch phenomenon. The mathematical model is promising for the use in a wider range of SWATH motion predictions, especially if more experimental data on other SWATH configurations could be made available for further verification.

REFERENCES

1. Lamb, G.R.(1988)," Some Guidance for Hull Form Selection for SWATH ships", Marine Technology, SNAME, Vol.25, No.4,Oct.
2. Djatmiko, E.B. (1996), "On the Prediction of SWATH Ship Motions in Regular Waves", Proc. Of 2nd Japan Indonesia Forum in Ocean Engineering, Surabaya, Sept.
3. Nordenstrom, M. (1973)," A Method to Predict Long-Term Distribution of Wave- Induced Motion and Loads on Ships and Other Floating Structures", Reseach Report, Publ .81, Det Norske Veritas, April.
4. Lee, C.M and Curphey, R.M (1977), "Prediction of Motion, Stability, and Wave Load of Small Waterplane –Area, Twin – Hull Ships", Transaction of SNAME, Vol.85.
5. Hong, Y.S. (1986), "Heave and Pitch Motion of SWATH Ship Reseach, SNAME, Vol.30, No.1, March.
6. Fang, M.C. (1988), " The Motion of SWATH ship in Waves", Journal of Ship Reseach, SNAME, Vol. 32, No.4, Dec.
7. Kobayashi M, Shimada. K, and Nishimura. K. (1990),"Wave Loads and Semi-Submerged Catamaran (SSC) with Forward Speed", Journal of Society of Naval Architect Japan, SNAJ, Vol.168.
8. Frank, W. (1976)," On the Oscilation of Cylinders in or below the Free Surface of Deep Fluids", NSRDC, Report No .2375.
9. Atlar, M. (1985), "Method for Predicting First Order Hydrodynamic Loads on Single and Twin section by Frank Close-Fit technique", Departmental Report, No. NAOE-85-41, Dept. of NAOE, Univ.of Glasgow, UK.
10. Djatmiko, E.B. (1987), "Experimental Investigation Into SWATH Ship Motion and Loadings", Master Thesis, Departement of Naval Architecture and Ocean Engineering, University of Glasgow, November.